NSG 87

UNPUBLISHED PRELIMINARY DATA

17P

SMITHSONIAN INSTITUTION
ASTROPHYSICAL OBSERVATORY

N64-26592
Code-1 Cat. 12
nasa Cr-58032

Research in Space Science

SPECIAL REPORT

Number 157

ATMOSPHERIC DENSITIES AND TEMPERATURES FROM THE DRAG ANALYSIS OF THE EXPLORER 17 SATELLITE

by

Jack Slowey

OTS PRICE

XEROX $ 1.60 ph.
MICROFILM $ _____

July 1, 1964

CAMBRIDGE, MASSACHUSETTS 02138

REPORTS CONTROL No. _____

SAO Special Report No. 157

ATMOSPHERIC DENSITIES AND TEMPERATURES FROM THE DRAG ANALYSIS OF THE EXPLORER 17 SATELLITE

by

Jack Slowey

July 1, 1964

Smithsonian Institution
Astrophysical Observatory
Cambridge, Massachusetts 02138

ATMOSPHERIC DENSITIES AND TEMPERATURES FROM THE DRAG ANALYSIS OF THE EXPLORER 17 SATELLITE[1]

Jack Slowey[2]

26592

Abstract.--Atmospheric densities were obtained from the drag analysis of the Explorer 17 satellite in the interval from April 8, 1963 to October 9, 1963. We computed temperatures from the densities, using a modified version of Nicolet's (1961) atmospheric model. The analysis was based on field-reduced Baker-Nunn observations and on Minitrack observations. A study of the preliminary results reveals that:

(a) The density in Nicolet's model corresponding to a given exospheric temperature is, relative to the densities higher up, too large at low heights. The same result was found in an earlier analysis of the Injun 3 satellite.

(b) Irregular fluctuations in density, with a range corresponding to 30°-40° in temperature, occur during geomagnetically quiet intervals. These fluctuations are correlated with small variations in the average K_p geomagnetic index.

(c) The heating that accompanies smaller magnetic storms may be considerably greater than previous results have indicated. The increase in temperature may very well be proportional to K_p, rather than to a_p, for K_p equal to 6 or more.

author

1. General

Explorer 17 (1963 ζ1) was launched on April 3, 1963, in an orbit having an eccentricity of 0.05, an inclination of 57°6 and a mean perigee height of about 270 km. Known as the "atmospheric structure satellite," Explorer 17 contained instruments to measure several physical quantities important to our knowledge of the earth's upper atmosphere. Among these was a pressure gauge, from which atmospheric densities could be determined. The primary purpose of this paper is to present densities obtained from the analysis of the atmospheric drag on Explorer 17 for comparison with those obtained from the direct measurements. The results, based on an analysis of field-reduced Baker-Nunn observations and Minitrack observations, are preliminary. Better resolution will be possible when the precisely reduced Baker-Nunn observations become available.

---

[1]This work was supported in part by grant NsG 87-60 from the National Aeronautics and Space Administration.

[2]Astronomer, Smithsonian Astrophysical Observatory.

Although the active life of Explorer 17 ended about July 10, 1963, in order to provide more complete coverage of the several sources of slow variation, we continued analysis of the drag until October 9.

2. Densities and temperatures

The methods used to determine orbital acceleration and to compute densities were essentially the same as those previously described by Jacchia and Slowey (1963a). Densities were computed by numerical integration of Sterne's integral in the form that includes the effect of atmospheric rotation (Sterne, 1958, 1959). The empirical atmospheric model previously used in the integration (Jacchia and Slowey, 1963a, 1964a) was, however, replaced with the latest version of Nicolet's (1961) model--referred to as Nicolet II in an earlier paper (Jacchia and Slowey 1964a). This model was used in combination with Jacchia's (1964) model for the diurnal temperature variation. Since Nicolet's model tabulates density as a function of exospheric temperature, and since the exact temperature could not be known beforehand, it was necessary to proceed by iteration. We obtained an initial temperature from the known relation between the temperature and the 10.7-cm solar flux (Jacchia, 1964), taking a mean value of the flux. To obtain a better value of the temperature we then entered in the model the computed density at each point and repeated the computation. A single iteration of this kind was sufficient.

Explorer 17 is a nearly spherical object, 35 inches in diameter. The mean presentation area, computed from drawings supplied by NASA, is 6597 cm^2. Since the mass of the satellite, according to NASA, is 1.855×10^5 grams, the area-to-mass ratio is .0356 cm^2/g. The drag coefficient, as usual, was taken to be 2.2.

The results of the analysis, together with other pertinent parameters, are given in Table 1 as a function of the time in Modified Julian Days (JD - 2400000.5); time is listed in the first column. Tabulation is at 1-day intervals except during magnetic storms, when the interval is 0.2 day. The gap of 9 days following MJD 38258 was the result of a scarcity of observations in that interval. The observed rate of change of the anomalistic period is given in the second column. The correction for the effect of solar radiation pressure, for which the third column is reserved, can be ignored at this height; for this reason column three is blank. The "corrected" value of dP/dt in column four, from which the density was computed, is just the rounded value from column two. The common logarithms of the perigee density, in gm/cm^3, at perigee height and at a standard height of 270 km are listed in columns five and six. We used Nicolet's model to make the reduction to standard height. The exospheric temperature at perigee, computed from Nicolet's model, is given in column seven. The next three columns give, in order, the perigee height, the difference in right ascension between perigee and the sun, and the difference in declination between perigee and the sun. The last column gives the nighttime temperature computed from the perigee value by use of Jacchia's model of the diurnal variation.

The logarithm of the standard perigee density and the corresponding exospheric temperature from Nicolet's model are plotted in Figure 1. Normalized curves of the diurnal and semiannual variations and plots of the 10.7-cm solar flux and the daily geomagnetic index A_p are shown for comparison.

3. Irregular variations in density during geomagnetically quiet intervals

The temperature at perigee is again plotted at the top of Figure 2. The three strips below it show the result of successively eliminating the diurnal variation, the semiannual variation, and the variation correlated with the decimetric solar flux by means of Jacchia's (1964) model for these variations. Specifically, the temperature plotted in the last of these strips is the nighttime exospheric temperature corrected for the semiannual variation and reduced to a mean value of the 10.7-cm solar flux $\bar{F}_{10.7} = 81 \times 10^{-22}$ watts/m^2/cycle/sec bandwidth. Perturbations related to magnetic storms have been excluded from this strip.

The "corrected" temperatures plotted in Figure 2 reveal several things. In the first place, the temperatures are systematically lower than would be expected from Nicolet's model at greater heights. This confirms the result from the Injun 3 satellite reported earlier (Jacchia and Slowey, 1964a). The average temperature from Figure 2 near July 1, when the perigee was actually quite close to the nighttime minimum is about 635°. This corresponds to an observed density of 1.5×10^{-14} g/cm^3 at 270 km. On the other hand, the relationship between the nighttime value of the temperature and the 10.7-cm flux determined by Jacchia (1964) from higher satellites gives a temperature of 704° for $\bar{F}_{10.7} = 81$. The corresponding density from Nicolet's model is 2.1×10^{-14} g/cm^3 or 1.4 times the observed value. Densities in the model appear to be significantly higher, relatively, than they should be at low heights.

Figure 2 also indicates a slight overcorrection for the diurnal variation. Since Jacchia's model has been quite successful in reducing the diurnal variation for other satellites, we assume that this overcorrection results from an incorrect variation of $d\rho/dT$ with height in Nicolet's model. Quantitatively, if the result of the previous paragraph is taken into account, the difference in amplitude is about 40°, or nearly 20 percent, in the temperature.

The most interesting thing about Figure 2, however, is that it clearly reveals irregular fluctuations in temperature that are not accounted for by the other variations. These fluctuations have a characteristic time on the order of 10 days and an average temperature range of 30°-40°, corresponding to a variation of 15-20 percent in the density at perigee. They are correlated with variations in the K_p geomagnetic index (Jacchia and Slowey, 1964b). Figure 3 shows temperatures from Explorer 8 and Injun 3 reduced in the same way as in figure 2 and plotted with the Explorer 17 results and the (two-day) average of the three-hourly K_p index. The fluctuations are essentially identical in the curves of all three satellites and, as well as can be determined, proportional to the K_p index. The constant of proportionality, $\Delta T/\Delta K_p$, is about 40°.

4. Heating during magnetic storms

Although 12 perturbations associated with larger geomagnetic disturbances were detected, adequate resolution could be obtained for only 10 of these. For each of the 10, the temperature outside the perturbation was corrected to $K_p = 0$, and the increase in temperature, ΔT, at maximum was determined. The values of ΔT are listed with the corresponding maximum values of K_p and a_p in Table 2.

Most of the disturbances were of moderate intensity; in only three cases was $K_p > 6$ at maximum. These smaller storms give values of $\Delta T/\Delta a_p$ between 2° and 4°--considerably higher than the $1^\circ.0$ or $1^\circ.2$ that would have been expected from previous results (Jacchia and Slowey, 1963b) assuming a linear relationship between ΔT and the a_p index. Indeed, the temperature increase seems to be nearly proportional to the K_p index for values up to $K_p = 6$ or more. The temperature increase for the 10 storms is plotted as a function of the maximum K_p in Figure 4. A value of $\Delta T/\Delta K_p$ on the order of 30° is indicated--not too much different from the value during unperturbed intervals quoted above. The value here would be increased somewhat if the fact that the resolution in the temperature is lower than that in K_p were taken into account. It should be emphasized, however, that proportionality with the K_p index does not hold for large storms; in this case the increase in temperature is more nearly proportional to the a_p index (see Jacchia and Slowey, 1964b).

References

JACCHIA, L. G.

1964. The temperature above the thermopause. Smithsonian Astrophys. Obs. Special Report No. 150, 32 pp.

JACCHIA, L. G., and SLOWEY, J.

1963a. Accurate drag determinations for eight artificial satellites; atmospheric densities and temperatures. Smithsonian Contr. Astrophys., vol. 8, No. 1, p. 1-99.

1963b. An analysis of the atmospheric drag of the Explorer IX satellite from precisely reduced photographic observations. Smithsonian Astrophys. Obs. Special Report No. 125, 57 pp.

1964a. Atmospheric heating in the auroral zones: a preliminary analysis of the atmospheric drag of the Injun 3 satellite. Journ. Geophys. Res., vol. 69, p. 905-910.

1964b. Temperature variations in the upper atmosphere during geomagnetically quiet intervals. Smithsonian Astrophys. Obs. Special Report No. 152, 7 pp.

NICOLET, M.

1961. Density of the heterosphere related to temperature. Smithsonian Astrophys. Obs. Special Report No. 75, 30 pp.

STERNE, T. E.

1958. An atmospheric model, and some remarks on the inference of density from the orbit of a close earth satellite. Astron. Journ., vol. 63, p. 81-87.

1959. Effect of the rotation of a planetary atmosphere upon the orbit of a close satellite. Journ. Amer. Rocket Soc., vol. 29, p. 777-782.

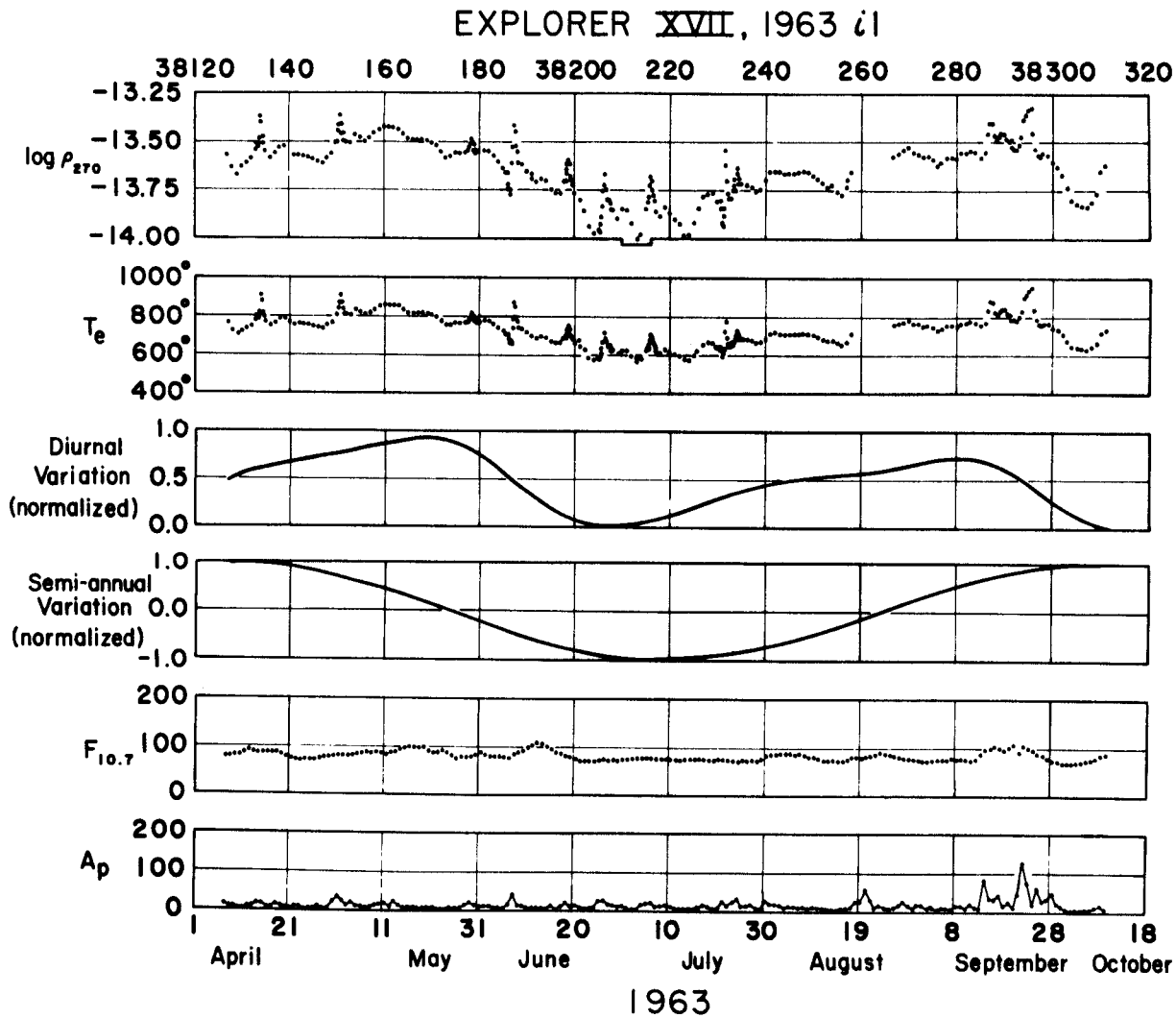

Figure 1.--Logarithms of the atmospheric densities determined from the drag analysis of the Explorer 17 satellite reduced to a standard height of 270 km (first strip) and the corresponding exospheric temperatures from Nicolet's model (second strip). Normalized curves of the diurnal variation and the semiannual variation and plots of the 10.7-cm solar flux (units of 10^{-22} watts/m^2/cycle/sec bandwidth) and A_p geomagnetic index are shown for comparison.

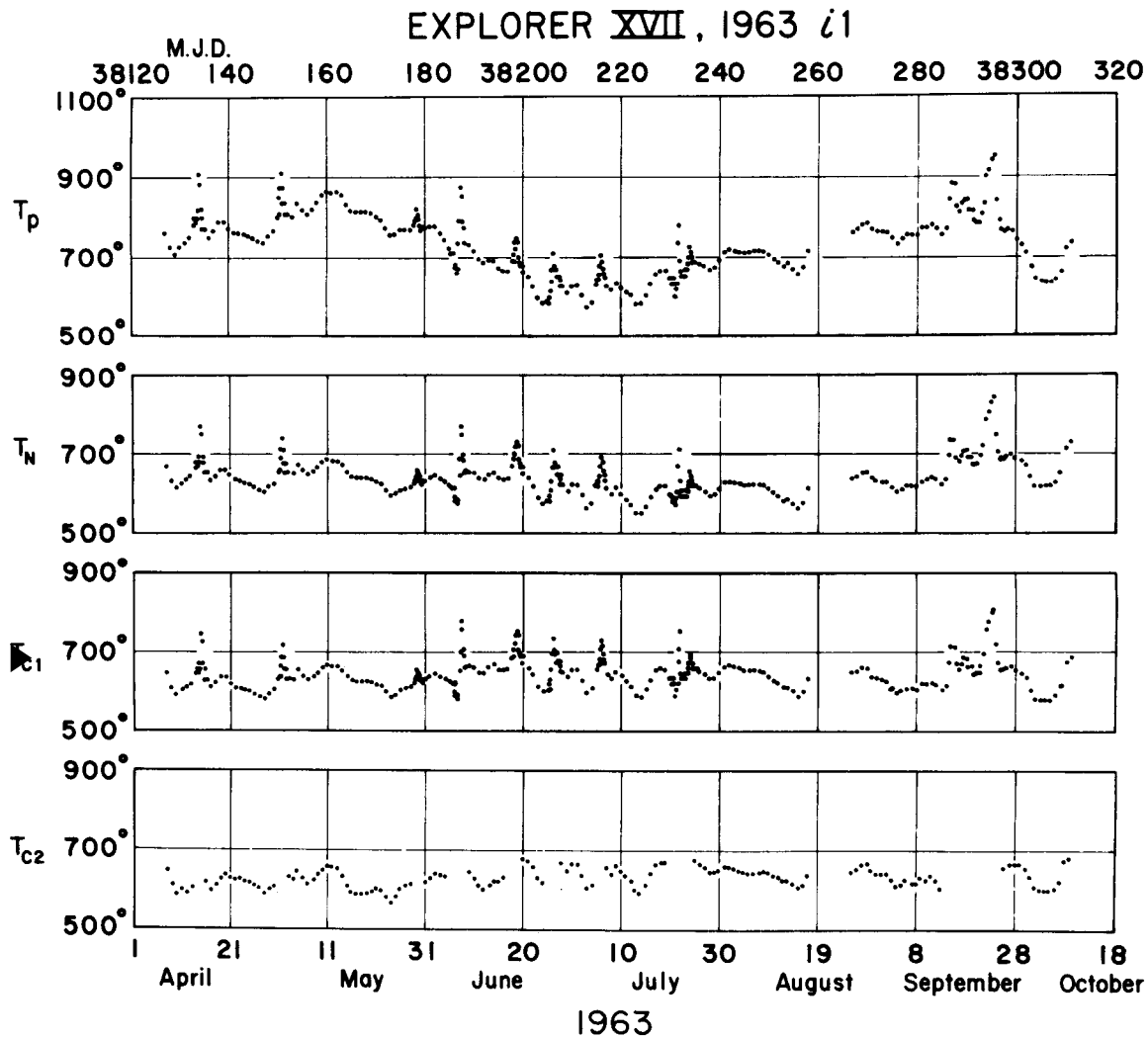

Figure 2.--The exospheric temperature at perigee from Nicolet's model for Explorer 17 (first strip) showing the result of successively eliminating the diurnal variation (second strip), the semiannual variation (third strip) and the variation with the decimetric solar flux (bottom strip). Perturbations related to magnetic storms have been excluded from the bottom strip.

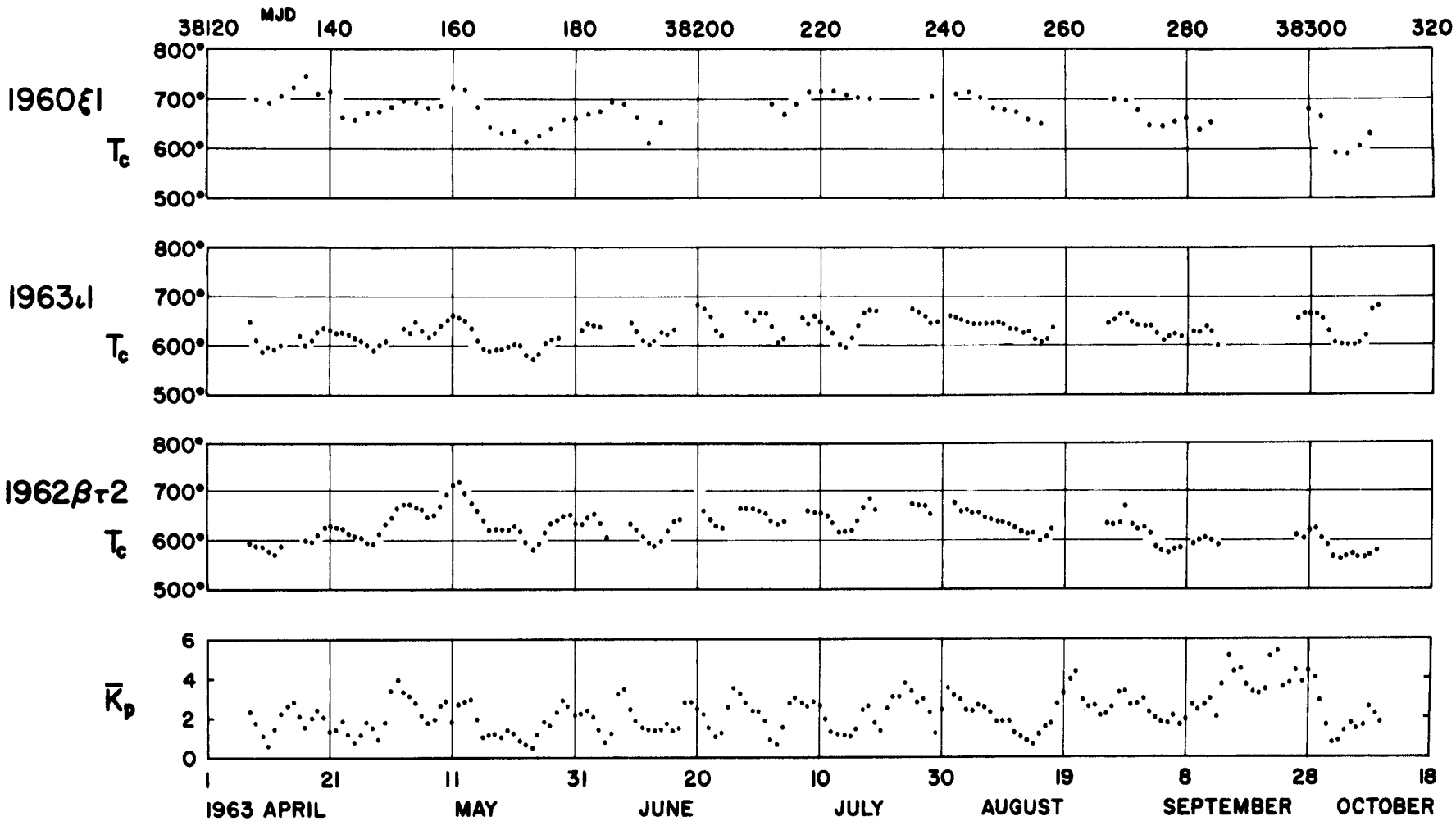

Figure 3.--Exospheric temperatures determined from Explorer 8 (1960 ξ1, perigee height 426 km), Explorer 17 (1963 ι1 , perigee height 270 km) and Injun 3 (1962 βτ2, perigee height 250 km) reduced in the same way as in Figure 2. The two-day running mean of the three-hourly geomagnetic index, K_p, is plotted in the bottom strip.(From Jacchia and Slowey, 1964b.)

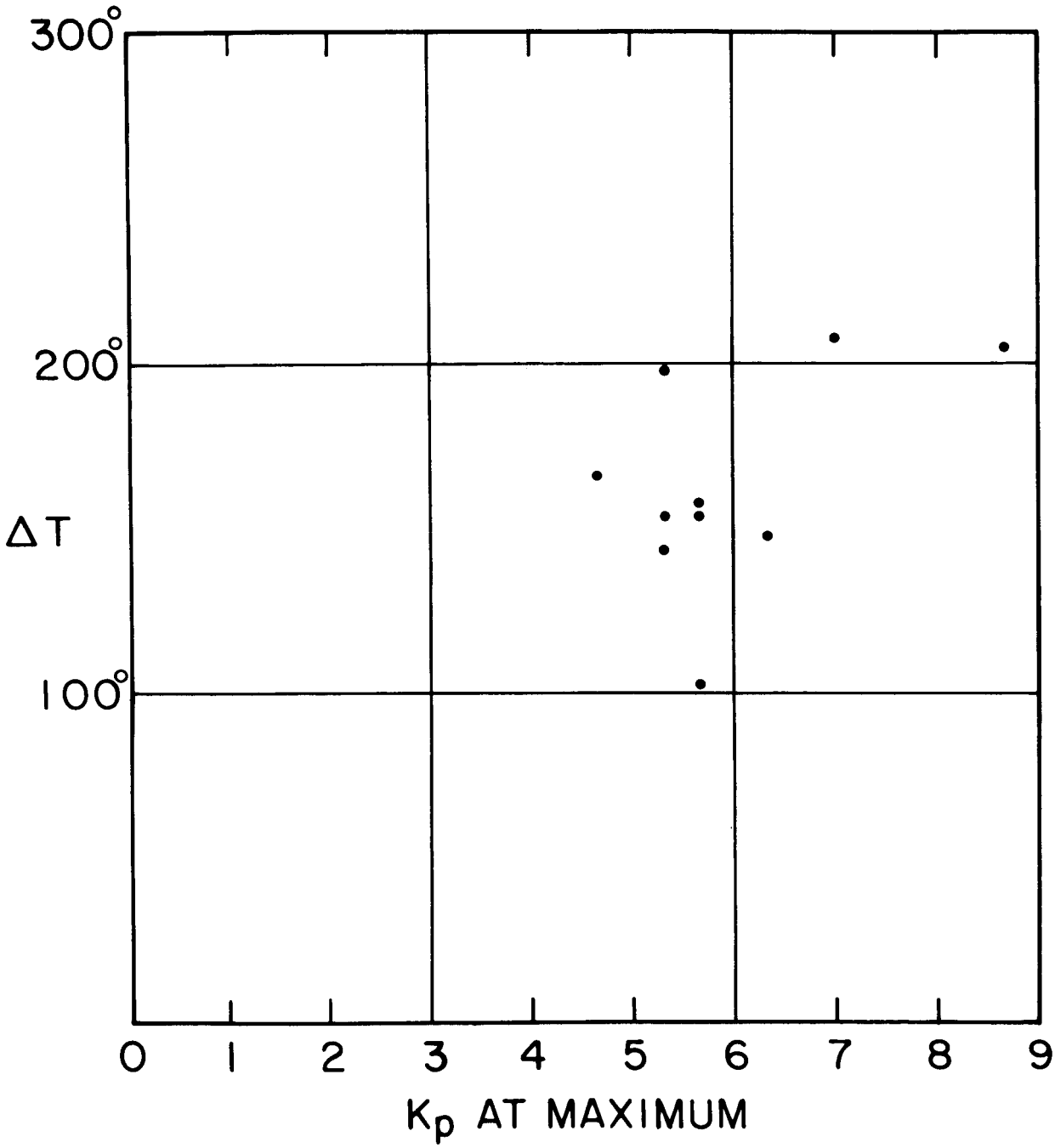

Figure 4.--The temperature increase at maximum during magnetic storms as a function of the corresponding maximum in the K_p geomagnetic index. The plotted points represent the data of Table 2.

Table 1.--Acceleration, drag, atmospheric densities, atmospheric temperature, and geometric parameters

MJD	$-10^6\ \dot{P}$	$-10^6\ \dot{P}_R$	$-10^6\ P_A$	$\log \rho_\pi$	$\log \rho_s$	T_π (°K)	z (km)	$\alpha_\pi-\alpha_\odot$	$\delta_\pi-\delta_\odot$	T_N (°K)
38127.0	2.65		2.6	-13.43	-13.57	764	259.2	127.1	38.5	668
28.0	2.25		2.2	.49	.63	727	259.6	124.0	39.1	632
29.0	2.05		2.0	.53	.67	709	259.9	120.9	39.6	613
30.0	2.22		2.2	.50	.63	728	260.2	117.8	40.2	627
31.0	2.32		2.3	.48	.61	739	260.5	114.8	40.7	634
32.0	2.43		2.4	.47	.59	752	260.8	111.9	41.2	642
33.0	2.75		2.7	.42	.53	785	261.1	109.1	41.7	668
38133.2	2.93		2.9	-13.40	-13.51	800	261.1	108.5	41.8	680
33.4	2.81		2.8	.41	.53	790	261.2	108.0	41.9	671
33.6	2.91		2.9	.40	.51	800	261.3	107.4	42.0	679
33.8	3.13		3.1	.37	.48	819	261.3	106.9	42.1	695
34.0	4.13		4.1	.27	.37	910	261.4	106.3	42.1	771
34.2	3.78		3.8	.30	.40	883	261.4	105.8	42.2	748
34.4	3.10		3.1	.37	.48	821	261.5	105.2	42.3	694
34.6	2.87		2.9	.40	.51	802	261.5	104.7	42.4	678
34.8	2.64		2.6	.44	.55	773	261.6	104.2	42.5	653
35.0	2.63		2.6	.44	.55	774	261.6	103.6	42.5	653
38136.0	2.40		2.4	-13.47	-13.58	756	261.9	101.0	42.9	636
37.0	2.53		2.5	.45	.56	770	262.1	98.5	43.2	646
38.0	2.71		2.7	.43	.53	789	262.3	96.0	43.5	660
39.0	2.72		2.7	.43	.52	792	262.5	93.6	43.8	660
40.0	2.53		2.5	.46	.55	774	262.7	91.2	43.9	644
41.0	2.41		2.4	.47	.57	763	262.9	89.0	44.1	633
42.0	2.40		2.4	.48	.57	764	263.0	86.8	44.2	632
43.0	2.37		2.4	.48	.57	762	263.1	84.6	44.2	629
44.0	2.32		2.3	.49	.58	758	263.2	82.5	44.2	624
45.0	2.24		2.2	.50	.59	750	263.3	80.4	44.1	616
46.0	2.18		2.2	.51	.60	745	263.4	78.4	43.9	610
47.0	2.11		2.1	.52	.61	738	263.4	76.4	43.7	604
48.0	2.29		2.3	.49	.58	757	263.4	74.4	43.4	618
49.0	2.40		2.4	.47	.56	769	263.4	72.4	43.1	626
50.0	2.77		2.8	.42	.50	807	263.3	70.4	42.7	655
38150.2	2.84		2.8	-13.41	-13.50	810	263.3	70.0	42.6	658
50.4	3.18		3.2	.36	.44	848	263.3	69.6	42.5	689
50.6	3.53		3.5	.33	.41	876	263.3	69.2	42.5	711
50.8	3.87		3.9	.29	.37	913	263.3	68.8	42.4	740
51.0	3.55		3.5	.33	.41	876	263.3	68.3	42.3	710
51.2	3.11		3.1	.37	.46	839	263.2	67.9	42.2	680
51.4	3.12		3.1	.37	.46	839	263.2	67.5	42.1	679
51.6	2.80		2.8	.41	.50	810	263.2	67.1	42.0	655
51.8	2.81		2.8	.41	.50	810	263.2	66.7	41.9	655
52.0	2.82		2.8	.41	.50	810	263.2	66.3	41.7	655
38153.0	2.75		2.7	-13.42	-13.50	804	263.0	64.2	41.2	649
54.0	3.08		3.1	.37	.46	836	262.9	62.0	40.5	673
55.0	2.93		2.9	.39	.48	821	262.7	59.8	39.8	659
56.0	2.84		2.8	.40	.49	811	262.5	57.6	39.1	650
57.0	2.97		3.0	.38	.48	823	262.3	55.3	38.3	657
58.0	3.16		3.2	.36	.46	839	262.0	52.9	37.5	669
59.0	3.38		3.4	.33	.43	858	261.8	50.4	36.6	682
60.0	3.49		3.5	.32	.42	866	261.4	47.8	35.6	687
61.0	3.47		3.5	.32	.43	862	261.1	45.2	34.6	682
62.0	3.51		3.5	.31	.42	863	260.8	42.5	33.6	681
63.0	3.44		3.4	.32	.44	854	260.4	39.7	32.6	673
64.0	3.28		3.3	.33	.46	834	259.7	36.9	31.5	656
65.0	3.11		3.1	.35	.49	818	259.5	34.0	30.4	642
66.0	3.11		3.1	.35	.49	817	259.4	30.9	29.2	640

MJD	$-10^6 \dot{P}$	$-10^6 \dot{P}_R$	$-10^6 P_A$	$\log \rho_\pi$	$\log \rho_s$	T_π (°K)	z (km)	$\alpha_\pi - \alpha_\odot$	$\delta_\pi - \delta_\odot$	T_N (°K)
38167.0	3.12		3.1	-13.35	-13.49	817	259.2	27.8	28.1	639
68.0	3.12		3.1	.35	.49	816	259.1	24.7	26.9	638
69.0	3.10		3.1	.35	.49	813	258.9	21.4	25.7	636
70.0	3.03		3.0	.36	.50	805	258.7	18.1	24.4	630
71.0	2.95		2.9	.37	.52	796	258.5	14.8	23.2	623
72.0	2.75		2.7	.40	.55	775	258.3	11.4	21.9	608
73.0	2.58		2.6	.42	.58	758	258.1	7.9	20.7	596
74.0	2.61		2.6	.42	.58	759	257.8	4.4	19.4	599
75.0	2.75		2.7	.39	.56	771	257.6	0.8	18.1	610
76.0	2.76		2.8	.39	.56	770	257.4	357.2	16.7	612
77.0	2.79		2.8	.39	.56	771	257.2	353.6	15.4	616
38177.8	2.86		2.9	-13.37	-13.54	780	257.0	350.6	14.4	626
78.0	2.97		3.0	.36	.53	789	256.9	349.9	14.1	634
78.2	3.08		3.1	.35	.51	798	256.9	349.2	13.8	642
78.4	3.30		3.3	.32	.49	815	256.9	348.4	13.6	657
78.6	3.18		3.2	.33	.50	806	256.8	347.7	13.3	651
78.8	3.06		3.1	.35	.52	797	256.8	346.9	13.0	644
79.0	2.95		2.9	.37	.54	778	256.7	346.2	12.7	630
79.2	2.83		2.8	.39	.56	769	256.7	345.4	12.5	623
79.4	2.94		2.9	.37	.55	778	256.6	344.7	12.2	631
38180.0	2.89		2.9	-13.37	-13.55	776	256.5	342.4	11.4	632
81.0	2.93		2.9	.37	.55	778	256.3	338.6	10.0	639
82.0	2.93		2.9	.37	.55	776	256.1	334.8	8.7	644
83.0	2.78		2.8	.39	.57	761	255.9	330.9	7.3	637
84.0	2.61		2.6	.41	.60	744	255.7	327.0	6.0	629
85.0	2.43		2.4	.44	.64	726	255.5	323.1	4.6	620
38185.6	2.28		2.3	-13.46	-13.66	713	255.4	320.7	3.8	613
85.8	2.28		2.3	.46	.66	713	255.4	320.0	3.5	614
86.0	2.27		2.3	.46	.66	712	255.4	319.2	3.2	616
86.2	2.04		2.0	.51	.72	683	255.3	318.4	2.9	591
86.4	1.92		1.9	.53	.74	672	255.3	317.6	2.7	584
86.6	1.79		1.8	.56	.77	662	255.3	316.8	2.4	576
86.8	1.90		1.9	.53	.74	672	255.2	316.0	2.1	586
87.0	2.56		2.6	.41	.61	739	255.2	315.2	1.8	646
87.2	3.22		3.2	.33	.52	793	255.2	314.4	1.6	694
87.4	4.21		4.2	.23	.41	877	255.1	313.6	1.3	770
87.6	3.87		3.9	.26	.44	852	255.1	312.8	1.0	750
87.8	3.19		3.2	.33	.52	792	255.1	312.0	0.7	699
88.0	2.96		3.0	.36	.55	774	255.1	311.2	0.5	684
88.2	2.61		2.6	.41	.61	738	255.0	310.4	0.2	654
88.4	2.60		2.6	.41	.61	738	255.0	309.6	-0.1	655
38189.0	2.56		2.6	-13.42	-13.62	734	254.9	307.2	-0.9	656
90.0	2.39		2.4	.44	.65	717	254.8	303.2	-2.3	648
91.0	2.19		2.2	.48	.69	698	254.8	299.1	-3.7	638
92.0	2.10		2.1	.49	.71	689	254.7	295.1	-5.0	636
93.0	2.17		2.2	.48	.70	695	254.6	291.0	-6.4	649
94.0	2.15		2.1	.48	.70	693	254.6	286.9	-7.8	653
95.0	1.94		1.9	.52	.74	672	254.6	282.8	-9.1	639
96.0	1.86		1.9	.54	.76	664	254.6	278.7	-10.5	636
97.0	1.84		1.8	.55	.76	664	255.0	274.6	-11.9	641
38197.8	2.07		2.1	-13.49	-13.71	691	255.0	271.3	-13.0	670
98.0	2.06		2.1	.49	.70	691	255.0	270.5	-13.3	671
98.2	2.27		2.3	.46	.67	710	255.0	269.7	-13.5	691
98.4	2.37		2.4	.44	.65	720	255.1	268.8	-13.8	701
98.6	2.58		2.6	.41	.61	738	255.1	268.0	-14.1	720

MJD	$-10^6\ \dot{P}$	$-10^6\ \dot{P}_R$	$-10^6\ P_A$	$\log \rho_\pi$	$\log \rho_s$	T_π (°K)	z (km)	$\alpha_\pi-\alpha_\odot$	$\delta_\pi-\delta_\odot$	T_N (°K)
38198.8	2.68		2.7	-13.40	-13.60	747	255.1	267.2	-14.4	729
99.0	2.56		2.6	.41	.61	738	255.1	266.4	-14.6	721
99.2	2.21		2.2	.48	.68	701	255.1	265.5	-14.9	686
99.4	2.09		2.1	.49	.70	692	255.2	264.7	-15.2	677
99.6	1.96		2.0	.51	.72	682	255.2	263.9	-15.4	668
99.8	1.95		2.0	.51	.72	682	255.2	263.1	-15.7	669
38200.0	1.82		1.8	.55	.76	664	255.2	262.2	-16.0	651
38201.0	1.67		1.7	-13.58	-13.80	649	255.4	258.1	-17.3	639
02.0	1.46		1.5	.64	.85	625	255.5	254.0	-18.7	618
03.0	1.20		1.2	.71	.94	593	255.7	249.8	-20.1	588
04.0	1.10		1.1	.75	.97	581	256.0	245.7	-21.4	577
05.0	1.11		1.1	.75	.96	584	256.2	241.5	-22.7	580
38205.2	1.13		1.1	-13.75	-13.97	583	256.3	240.7	-23.0	580
05.4	1.23		1.2	.72	.93	597	256.3	239.9	-23.3	593
05.6	1.33		1.3	.68	.89	610	256.4	239.0	-23.5	607
05.8	1.55		1.5	.63	.83	635	256.4	238.2	-23.8	632
06.0	1.76		1.8	.56	.75	670	256.5	237.4	-24.1	666
06.2	2.20		2.2	.48	.66	711	256.6	236.6	-24.3	707
06.4	1.86		1.9	.54	.73	681	256.6	235.7	-24.6	678
06.6	1.85		1.8	.56	.75	671	256.7	234.9	-24.9	667
06.8	1.84		1.8	.56	.75	671	256.7	234.1	-25.1	668
07.0	1.61		1.6	.60	.80	649	256.8	233.2	-25.4	646
07.2	1.60		1.6	.60	.79	649	256.9	232.4	-25.7	647
07.4	1.60		1.6	.60	.79	650	256.9	231.6	-25.9	647
07.6	1.48		1.5	.63	.82	638	257.0	230.8	-26.2	636
07.8	1.36		1.4	.66	.85	626	257.1	229.9	-26.5	624
38208.0	1.39		1.4	-13.66	-13.85	625	257.1	229.1	-26.7	623
09.0	1.24		1.2	.71	.90	608	257.5	225.0	-28.0	605
10.0	1.37		1.4	.67	.85	627	257.9	220.8	-29.3	624
11.0	1.36		1.4	.67	.85	627	258.3	216.7	-30.6	624
12.0	1.14		1.1	.74	.92	600	258.7	212.6	-31.9	596
13.0	0.92		0.9	.83	-14.00	570	259.2	208.5	-33.2	565
14.0	0.97		1.0	.81	-13.97	580	259.7	204.4	-34.5	573
15.0	1.32		1.3	.69	.84	631	260.2	200.3	-35.8	622
38215.2	1.38		1.4	-13.67	-13.81	642	260.3	199.5	-36.0	633
15.4	1.37		1.4	.67	.81	643	260.4	198.6	-36.3	633
15.6	1.48		1.5	.64	.78	656	260.5	197.8	-36.5	645
15.8	1.70		1.7	.59	.73	680	260.6	197.0	-36.8	669
16.0	1.92		1.9	.55	.68	703	260.7	196.2	-37.0	691
16.2	1.81		1.8	.57	.70	693	260.8	195.4	-37.3	680
16.4	1.58		1.6	.62	.75	670	260.9	194.6	-37.5	658
16.6	1.47		1.5	.64	.77	659	261.0	193.8	-37.8	646
16.8	1.35		1.4	.67	.80	647	261.1	192.9	-38.0	633
38217.0	1.23		1.2	-13.72	-13.85	625	261.2	192.1	-38.3	611
18.0	1.13		1.1	.76	.88	613	261.8	188.1	-39.5	598
19.0	1.25		1.2	.72	.83	633	262.4	184.0	-40.8	615
20.0	1.15		1.1	.76	.86	622	263.0	180.0	-42.0	601
21.0	1.04		1.0	.80	.89	608	263.6	176.0	-43.2	585
22.0	0.96		1.0	.83	.92	599	264.3	172.0	-44.4	574
23.0	0.81		0.8	.90	.98	577	264.9	168.1	-45.6	550
24.0	0.80		0.8	.91	.98	578	265.6	164.1	-46.7	548
25.0	0.91		0.9	.86	.92	599	266.3	160.2	-47.9	566
26.0	1.06		1.1	.81	.84	629	267.5	156.3	-49.1	591
27.0	1.23		1.2	.75	.78	657	268.0	152.5	-50.2	614
28.0	1.27		1.3	.74	.76	665	268.6	148.7	-51.3	618

MJD	$-10^6 \dot{P}$	$-10^6 \dot{P}_R$	$-10^6 P_A$	$\log \rho_\pi$	$\log \rho_s$	T_π (°K)	z (km)	$\alpha_\pi - \alpha_\odot$	$\delta_\pi - \delta_\odot$	T_N (°K)
38229.0	1.26		1.3	-13.75	-13.76	666	269.2	144.9	-52.4	616
30.0	1.11		1.1	.80	.80	647	269.8	141.1	-53.5	595
38230.2	1.07		1.1	-13.80	-13.80	645	269.9	140.4	-53.7	594
30.4	1.07		1.1	.80	.80	646	270.0	139.6	-54.0	594
30.6	0.96		1.0	.84	.84	631	270.1	138.9	-54.2	579
30.8	0.96		1.0	.84	.84	631	270.2	138.1	-54.4	579
31.0	0.85		0.8	.93	.92	597	270.4	137.4	-54.6	548
31.2	0.85		0.9	.88	.88	615	270.5	136.7	-54.8	564
31.4	0.96		1.0	.84	.83	633	270.6	135.9	-55.0	579
31.6	1.74		1.7	.63	.62	732	270.7	135.2	-55.2	669
31.8	2.08		2.1	.55	.54	781	270.8	134.5	-55.4	713
32.0	1.41		1.4	.71	.70	694	271.0	133.7	-55.6	633
32.2	1.19		1.2	.77	.76	666	271.1	133.0	-55.9	607
32.4	1.08		1.1	.81	.79	651	271.2	132.3	-56.1	593
32.6	1.08		1.1	.81	.79	652	271.3	131.5	-56.3	593
32.8	1.08		1.1	.81	.79	652	271.4	130.8	-56.5	593
33.0	1.08		1.1	.81	.79	653	271.5	130.1	-56.7	593
33.2	1.19		1.2	.78	.75	669	271.7	129.4	-56.9	607
33.4	1.19		1.2	.78	.75	669	271.8	128.7	-57.1	607
33.6	1.31		1.3	.75	.72	684	271.9	127.9	-57.3	620
33.8	1.42		1.4	.72	.69	699	272.0	127.2	-57.5	633
34.0	1.64		1.6	.66	.63	726	272.1	126.5	-57.7	657
34.2	1.53		1.5	.69	.66	714	272.3	125.8	-57.9	645
34.4	1.42		1.4	.72	.68	701	272.4	125.1	-58.1	633
34.6	1.31		1.3	.75	.71	687	272.5	124.4	-58.3	620
34.8	1.31		1.3	.75	.71	688	272.6	123.7	-58.5	620
35.0	1.31		1.3	.75	.71	688	272.7	123.0	-58.7	620
38236.0	1.25		1.2	-13.77	-13.72	684	273.3	119.5	-59.7	613
37.0	1.20		1.2	.79	.73	679	273.9	116.1	-60.6	607
38.0	1.11		1.1	.82	.75	668	274.5	112.7	-61.5	595
39.0	1.13		1.1	.81	.74	674	275.1	109.4	-62.4	598
40.0	1.24		1.2	.78	.70	693	275.7	106.1	-63.3	614
41.0	1.37		1.4	.74	.66	715	276.2	103.0	-64.1	631
42.0	1.37		1.4	.74	.65	718	276.8	99.9	-65.0	632
43.0	1.33		1.3	.76	.66	715	277.3	96.8	-65.7	628
44.0	1.30		1.3	.77	.66	714	277.8	93.9	-66.5	625
45.0	1.27		1.3	.78	.66	712	278.4	91.0	-67.1	622
46.0	1.26		1.3	.78	.66	713	278.9	88.3	-67.8	622
47.0	1.26		1.3	.78	.65	716	279.3	85.6	-68.4	623
48.0	1.25		1.2	.79	.65	717	279.8	83.0	-69.0	623
49.0	1.22		1.2	.80	.66	715	280.2	80.5	-69.5	620
50.0	1.15		1.1	.82	.67	707	280.7	78.1	-69.9	612
51.0	1.07		1.1	.85	.69	698	281.3	76.0	-70.4	603
52.0	1.01		1.0	.87	.71	689	281.5	73.8	-70.7	595
53.0	0.94		0.9	.90	.73	677	281.7	71.7	-71.0	584
54.0	0.96		1.0	.89	.72	682	281.9	69.6	-71.2	588
55.0	0.88		0.9	.93	.75	668	282.0	67.7	-71.3	575
56.0	0.82		0.8	.95	.78	658	282.1	65.7	-71.3	565
57.0	0.90		0.9	.91	.74	674	282.2	63.8	-71.3	579
58.0	1.13		1.1	.82	.65	716	282.2	62.0	-71.2	614
38267.0	1.43		1.4	-13.72	-13.57	763	281.4	45.1	-66.7	642
68.0	1.48		1.5	.71	.56	770	281.2	43.0	-65.8	646
69.0	1.58		1.6	.68	.54	783	281.0	40.8	-64.9	655
70.0	1.61		1.6	.67	.53	786	280.7	38.6	-63.9	656
71.0	1.50		1.5	.70	.56	768	280.4	36.2	-62.9	639
72.0	1.49		1.5	.70	.57	765	280.1	33.8	-61.8	635

MJD	$-10^6 \dot{P}$	$-10^6 \dot{P}_R$	$-10^6 P_A$	$\log \rho_\pi$	$\log \rho_s$	T_π (°K)	z (km)	$\alpha_\pi - \alpha_\odot$	$\delta_\pi - \delta_\odot$	T_N (°K)
38273.0	1.48		1.5	-13.70	-13.57	762	279.8	31.3	-60.6	631
74.0	1.49		1.5	.70	.57	761	279.4	28.6	-59.4	629
75.0	1.41		1.4	.72	.60	747	279.1	25.9	-58.2	616
76.0	1.33		1.3	.74	.62	733	278.7	23.2	-56.9	603
77.0	1.43		1.4	.71	.60	745	278.3	20.3	-55.6	612
78.0	1.52		1.5	.69	.58	756	277.9	17.4	-54.2	620
79.0	1.54		1.5	.68	.58	756	277.4	14.4	-52.8	620
80.0	1.54		1.5	.68	.59	753	277.0	11.3	-51.4	617
81.0	1.70		1.7	.64	.55	772	276.5	8.1	-50.0	633
82.0	1.73		1.7	.63	.55	773	276.1	4.9	-48.5	634
83.0	1.80		1.8	.62	.54	779	275.6	1.7	-47.0	640
84.0	1.76		1.8	.62	.56	770	275.1	358.3	-45.5	634
85.0	1.67		1.7	.64	.58	755	274.6	355.0	-44.0	624
38286.0	1.75		1.8	-13.61	-13.56	769	274.1	351.5	-42.4	637
86.5	2.37		2.4	.50	.45	840	273.9	349.8	-41.6	698
87.0	2.84		2.8	.44	.40	883	273.6	348.0	-40.8	735
87.5	2.80		2.8	.44	.40	881	273.4	346.3	-40.0	735
88.0	2.53		2.5	.48	.47	827	270.3	344.9	-38.9	691
88.5	2.43		2.4	.49	.49	813	270.0	343.2	-38.1	681
89.0	2.59		2.6	.46	.46	833	269.7	341.4	-37.2	700
89.5	2.65		2.7	.44	.45	841	269.4	339.6	-36.4	709
90.0	2.67		2.7	.44	.46	839	269.1	337.8	-35.6	709
90.5	2.48		2.5	.47	.49	815	268.7	336.0	-34.8	692
91.0	2.46		2.5	.47	.49	813	268.4	334.1	-33.9	692
91.5	2.31		2.3	.50	.53	789	268.1	332.3	-33.1	674
92.0	2.27		2.3	.50	.53	787	267.8	330.5	-32.3	675
92.5	2.31		2.3	.50	.53	785	267.5	328.6	-31.4	676
93.0	2.46		2.5	.47	.50	804	267.2	326.8	-30.6	696
93.5	2.76		2.8	.42	.46	833	266.8	324.9	-29.7	724
94.0	3.47		3.5	.34	.38	900	266.5	323.0	-28.9	786
94.5	3.68		3.7	.32	.36	917	266.2	321.2	-28.0	804
95.0	4.00		4.0	.29	.33	943	265.9	319.3	-27.2	831
95.5	4.12		4.1	.28	.33	949	265.6	317.4	-26.3	841
96.0	2.95		3.0	.39	.45	842	265.3	315.5	-25.5	749
96.5	2.50		2.5	.46	.53	790	265.0	313.6	-24.6	706
97.0	2.26		2.3	.49	.56	767	264.7	311.7	-23.8	689
97.5	2.33		2.3	.49	.57	765	264.4	309.8	-22.9	691
38298.0	2.34		2.3	-13.49	-13.56	767	264.2	307.8	-22.0	696
99.0	2.34		2.3	.48	.57	764	263.6	304.0	-20.3	700
38300.0	2.19		2.2	.51	.60	745	263.0	300.1	-18.6	689
01.0	2.10		2.1	.52	.62	732	262.5	296.2	-16.8	684
02.0	1.93		1.9	.55	.66	711	262.0	292.3	-15.1	670
03.0	1.65		1.6	.61	.73	676	261.5	288.4	-13.4	644
04.0	1.42		1.4	.67	.80	646	261.0	284.4	-11.6	620
05.0	1.39		1.4	.68	.82	640	260.6	280.4	-9.9	619
06.0	1.38		1.4	.68	.82	637	260.1	276.5	-8.1	619
07.0	1.38		1.4	.68	.83	635	259.7	272.5	-6.4	621
08.0	1.46		1.5	.65	.81	643	259.3	268.5	-4.6	633
09.0	1.64		1.6	.61	.77	662	259.0	264.5	-2.8	655
10.0	2.21		2.2	.49	.64	721	258.6	260.5	-1.1	715
11.0	2.35		2.3	.46	.62	733	258.3	256.4	0.7	729

Table 2.--Explorer 17 - atmospheric and geomagnetic perturbations

MJD	ΔT	K_p (max)	a_p (max)
38134	166°	5-	39
150	148	6+	94
178	103	6-	67
187	208	7o	132
198	154	5+	56
206	158	6-	67
216	154	6-	67
231	198	5+	56
234	144	5+	56
295	205	9-	300